Possibility of Locking Compression Plate as the Treatment of External Fixation for Femoral Bone Based on Finite Element Method

Kriengkrai Nabudda [1], Jarupol Suriyawanakul [1,*], Kiatfa Tangchaichit [1], Weerachai Kosuwon [2], Kamolsak Sukhonthamarn [2], Nattadon Pannucharoenwong [3]

[1] Department of Mechanical Engineering, Faculty of Engineering, Khon Kaen University, Khon Kaen, Thailand;
Email: kriang.36@gmail.com (K.N.), kiatfa@kku.ac.th (K.T.)
[2] Department of Orthopaedic, Faculty of Medicine, Khon Kaen University, Khon Kaen, Thailand;
Email: weera_ko@kku.ac.th (W.K.), s.kamolsak@gmail.com (K.S.)
[3] Thammasat School of Engineering, Faculty of Engineering, Thammasat University Thailand;
Email: pnattado@engr.tu.ac.th (N.P.)
*Correspondence: jarupol@kku.ac.th (J.S.)

***Abstract*—This study aimed to evaluate the external fixation for femoral bone fracture by possibly using the 10-hole locking compression plates (LCPs). A comparison of LCPs, including 10-hole board LCP and 10-hole narrow LCP, was analyzed under femoral bone cutting at a 1 mm increment. The maximum load on 800 N, then, the structure was analyzed for dual LCP by making the implant model on the side lateral-anterior. The result of the study demonstrated that both board LCP and narrow LCP had the maximum stiffness above the maximum stress of the structure and greater than the ultimate tensile stress of 304-stainless steel. Recheck a board LCP model that was unable by torsion load on 12 Nm. Thus, increasing a board LCP on the side anterior of the femur, or dual LCP, was appropriated to treat femoral bone fracture as the external fixation because dual LCP can be the overall load.**

***Keywords*—finite element analysis (FEA), external fixation, locking compression plates (LCP), stiffness, treatment**

I. Introduction

The prognosis of femoral fracture surgical treatment is needed for the treatment methods that engineering principles use to help medical to ensure the accuracy and speed of the surgery both can select the appropriate equipment for the surgical treatment of external femoral fractures by locking compression plates (LCP). In the surgical treatment for fracture of the femoral bone, there are 3 types of fixation methods with a variety of equipment appropriate, including nails, commonly used to treat fractures inserted in the central canal of the long bone, plates, and screws, a usual implant which place on the bone surface, and external fixation included the pins that are drilled into the bone and linked to a metal bar which is set away from the fracture site on both ends of the fracture. The finite element analysis (FEA) could calculate the stiffness and assess the fixation models for femoral bone fracture.

External fixation could be a reliable treatment for the femur and tibia fractures and nonunion, which are associated with bone defects a method to calculate the stiffness of external fixation is compared with the Unilateral method because of a similar structure by there is stiffness of 107–126 N/mm. Therefore, the studies of LCP were more acceptable in those patients and might display favorable outcomes, especially in soft tissue or skin healing and infection resolution [1–5].

The locking compression plate (LCP) is used for internal fixation for various types of long bone fractures. A recent study demonstrated that the lateral-medial configuration of the dual plate of the 10-hole LCP had the highest stiffness at 715.41 N/mm [6].

The previous study exhibited the fresh femoral bone properties had Young's modulus and Poisson's ratio at 304.4756 MPa, and 0.3334, respectively, which the surrogate model identified. Therefore, these values of fresh femoral bone properties could be used to fit the external fixation of the femoral bone model [7]. Moreover, biomechanical testing for maximum stiffness in the construct rotation in the spinal instrument experiment could be applied [8]. Internal fixation with a lateral plate could provide successful outcomes in fractures with gaps [9]. Moreover, Chen *et al.* conducted FEA for spanning LCP in the periprosthetic femoral fracture, demonstrating that it could increase the local compressive stiffness [10]. Recent studies demonstrated that quantitative computed tomography and FEA could be used to investigate the mechanical characteristics of fractured distal femurs [11,12]. The computerized analysis as finite element models had improved fracture assessments of bone experiments from the literature and predicted the fracture load of bone [13–27]. Furthermore, FEA proceeded with

Manuscript received February 1, 2023; revised March 6, 2023; accepted April 3, 2023.

doi: 10.18178/ijmerr.12.5.290-296

the implant testing and vibration by calculating the natural frequency of the beam structure [28–30], and the structure has been analyzed by nonlinear to use for a composite structure which used FEA for structural analysis to failure [31–33].

Therefore, the study aimed to calculate the stiffness of 10-hole LCP as an external fixation for the femur and studied the possibility of determining the LCP applied to treat the external fixation method for the femoral bone fracture. There are 2 types of LCP to find strength is the best; the case studies have single LCL and dual LCP to find stiffness compared.

II. Materials and Methods

A. Material Property

The 10-hole broad LCPs with a dimension width of 17 mm, 186 mm in length, and a thickness of 6 mm were used to experiment. The distance between screw holes was 18 mm. The 10-hole narrow LCP was a width of 14 mm, a length of 192 mm, and a thickness of 6 mm, with the distance between screw holes at 20 mm. Screws had a head diameter of 5 mm, and a length of 130 mm. The models of femoral bone presented a height of 420 mm, and a diameter of the midshaft at 25 mm. Material properties had Poisson's ratio and Young's Modulus [6,7] for simulation in FEA was shown in Table I.

TABLE I. Material Properties are Used for Finite Element Analysis

Material	Poisson's ratio	Young's Modulus (MPa)
Screw (Stainless steel)	0.3100	200,000
LCP (Stainless steel)	0.3100	200,000
Femur bone	0.3334	304.4756

B. Finite Element Methods

The finite element method (FEM) is a numerical analysis technique for assessing approximate solutions to partial differential equations along with integral equations and the results are based on the differential equations. The mathematical integrations use standard mathematical techniques such as the Euler method and Runge Kutta methods to solve the differential equations. The partial differential equation is to create an equation that can approximate the equation of interest to study. This means that any discrepancies in the input and intermediate calculations will not be included and result in data output being meaningless. There are several methods available with different advantages and disadvantages. However, FEMs are a good choice for solving complex domains of differential equations.

$$E = \frac{\sigma}{\varepsilon} = \frac{P/A}{\delta/L} \tag{1}$$

$$E = \frac{G(3\lambda + 2G)}{\lambda + G} = \frac{\lambda(1+\nu)(1-2\nu)}{\nu} = 2G(1+\nu) \tag{2}$$

Hooke's law:

$$\varepsilon = \frac{1-2\nu}{E}(\sigma) \tag{3}$$

E = modulus of elasticity, σ = stress on cross-section, P = loading, A = cross section area, $\varepsilon = \frac{\delta}{L}$ elongation, δ = longitudinal deformation, L = length of the member, G = rigidity modulus, ν = Poisson's ratio.

This study conducted the boundary conditions, which were calculated according to the axial load by compression of 800 N on the proximal femur, with the construct of the fixed distal femur. The contact surface between the bone screw was bonding and the bonding set contact surface of a gap was frictionless. The mesh size analysis convergence on 4 mm of bone has a number of 77,738 elements. The process of simulation is shown in Fig. 1.

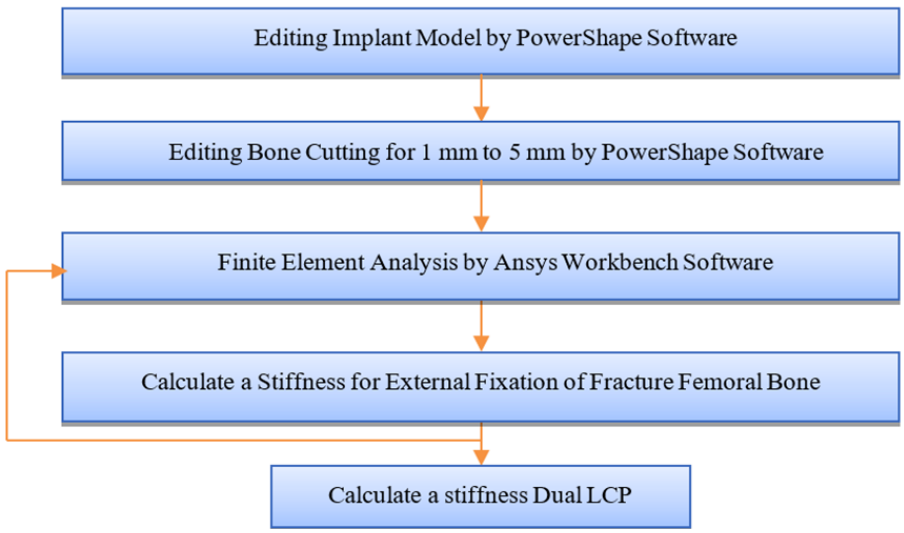

Figure 1. The workflow of the simulation.

C. External Fixation for the Femur

PowerShape software (Autodesk Inc., San Rafael, California, USA) generated the implant models. ANSYS workbench software (ANSYS Inc., Canonsburg, Pennsylvania, USA) was calculated for the stiffness of LCP-external fixation with the process workflow in Fig. 2.

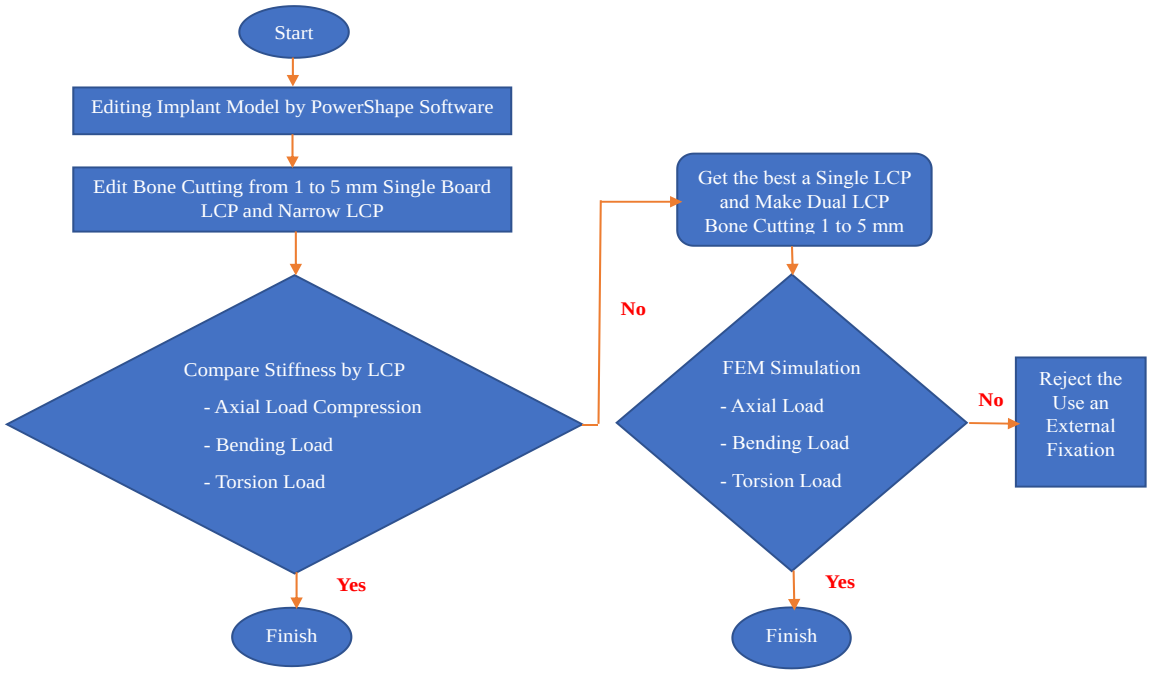

Figure 2. The workflow of the external fixation process by 10-hole LCP.

The Firstly has compared a stiffness type of LCP by bone cutting of 1 mm to 5 mm for compression load. Secondly, a simulation of a single LCP and dual LCP was performed for a torsional load to calculate stiffness, and test a 4-point bending load on the anterior-posterior, and lateral-medial for a bone gap of 3 mm because a maximum gap of bone able healing.

III. Result and Discussion

Broad LCP had a maximum stress of 321.81 MPa and a stiffness of 151.20 N/mm by the axial load on a gap of 1 mm. For a gap of 5 mm, the maximum stress and stiffness were 507.76 MPa and 84.89 N/mm, respectively. For a bone gap of 3 mm model by torsional load, the maximum stress occurred on the screw at 1033 MPa and the stiffness at 0.253 Nm/degree. On the side anterior-posterior bend, a 4-point bending load had maximum stress of 137.87 MPa, and stiffness at 261.45 N/mm. On the side lateral-medial bend, a 4-point bending load had the maximum stress at 386.75 MPa, and stiffness was 261.45 N/mm. The stiffness and maximum stress were 150.20 N/mm and 365.05 MPa, respectively, for narrow LCP from the axial load on a gap of 1 mm. While a gap of 5 mm has maximum stress of 630.37 MPa and stiffness was 84.34 N/mm. The stress of the structure was more than the ultimate tensile stress of 304 stainless steel, which was 586 MPa. A dual LCP at a bone gap of 3 mm has a stiffness on the side lateral-anterior for the axial load at 116.45 N/mm, stress was 258.95 MPa, torsional load stiffness was 378.55 N·mm/degree, maximum stress was 578.18 MPa, a 4-point bending load stiffness at 625.00 N/mm, and stress was 414.09 MPa on the side anterior-posterior bend. Moreover, a 4-point bending load had a stiffness of 421.05 N/mm, and stress was 476.3 MPa on the side lateral-medial bend.

A. Compare the Type of Locking Plate by Cutting off the Femur Bone

The dimension and configuration of external fixation for femoral bone were calculated for the stiffness by comparing the board LCP and narrow LCP of 10-hole LCP. A model was created in PowerShape software as shown in Fig. 3. For dual LCP testing, the distance between the screw holes on the plate was 36 mm. Therefore, the distance between screws purchased in the bone was 18 mm when double-LCP was applied to the model used for FEA in ANSYS workbench software shown in Fig. 4.

A board LCP had a von Misses stress less than a narrow LCP, which was the maximum stress of 507.76 MPa and 630.37 respectively on the femoral bone for a gap of 5 mm, the result occurs stress is more than the ultimate tensile stress of stainless steel 304 and identifies on a maximum gap of 5 mm for a narrow LCP model that structure was ability maximum load at 800 N as shown in Fig. 5.

A board LCP had a stiffness was 151.20 N/mm a narrow LCP had a stiffness was 150.20 N/mm on the femoral bone for a gap of 1 mm, the femoral bone gap of 5 mm a board LCP has a stiffness was 84.89 N/mm and a narrow LCP has a stiffness was 84.34 N/mm as shown in Fig. 6. As a result of identifying stiffness, thus as select board LCP to check torsion and 4-point bending load by a bone gap of 3 mm because a maximum bone for healing was a maximum gap of 3 mm [1] and stiffness had less than Unilateral method [2] compared with dual LCP model that was fixed on side lateral-anterior.

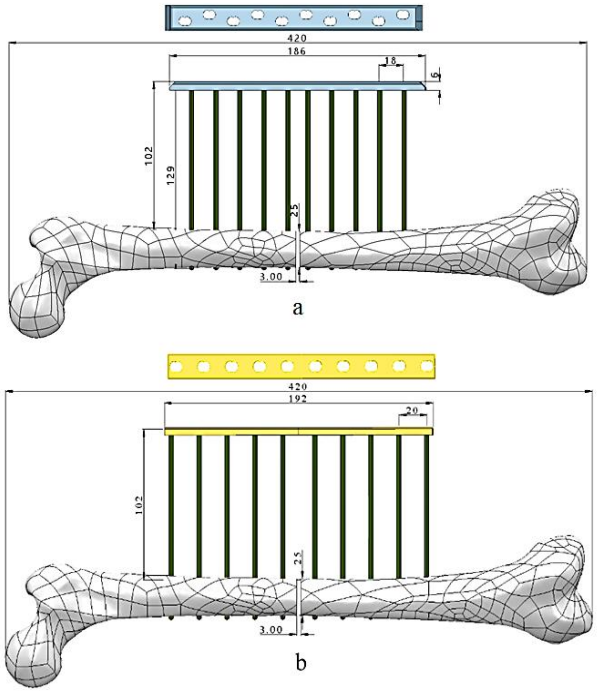

Figure 3. Models of the 10-hole LCP (a) board 10-hole LCP (b) narrow 10-hole LCP.

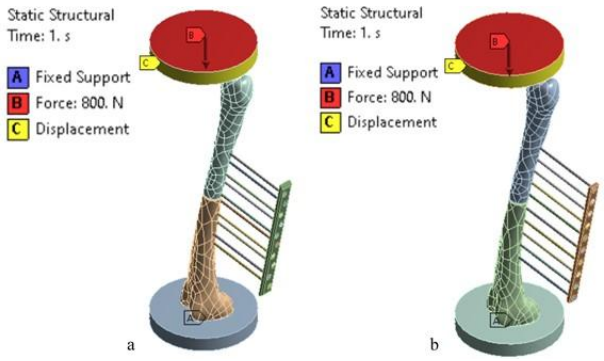

Figure 4. Shows boundary condition axial load at 800 N (a) board 10-hole LCP (b) narrow 10-hole LCP.

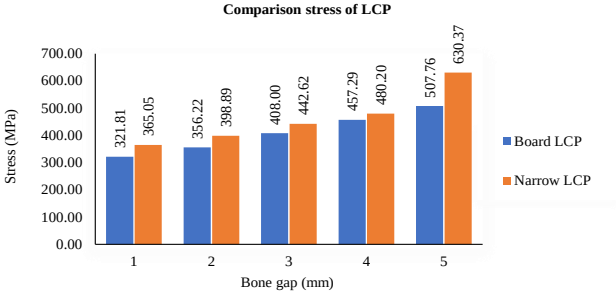

Figure 5. The comparison of the stress of the locking compression plate (LCP) for the femoral bone cutting off every 1 mm to a maximum load at 800 N.

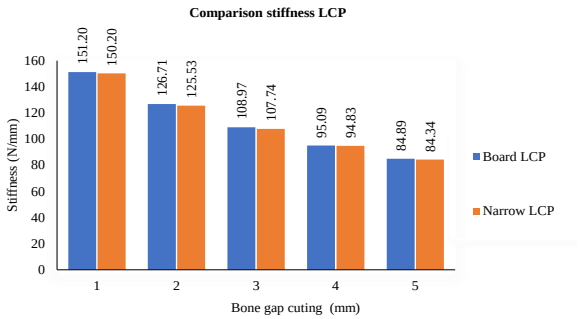

Figure 6. The comparison of the stiffness of the locking compression plate (LCP) for the femoral bone cutting off every 1 mm to 5 mm.

B. *Recheck Torsion Load and 4-point Bending Load*

The torsion load was applied at 12,000 N·mm for the proximal femur with the fixed distal femur for a femoral bone gap of 3 mm. A maximum rotation in a single LCP was 47.4 degrees and a maximum rotation in a dual LCP was 31.7 degrees shown in Fig. 7. The position of maximum stress in the first screw near the proximal occurs in both configurations, a single LCP had maximum stress of 1033 MPa and the maximum stress of a dual LCP was 578.2 MPa for a single LCP had stress more than the ultimate tensile stress of stainless steel 304 thus as the structure was a deformed shown in Fig. 8.

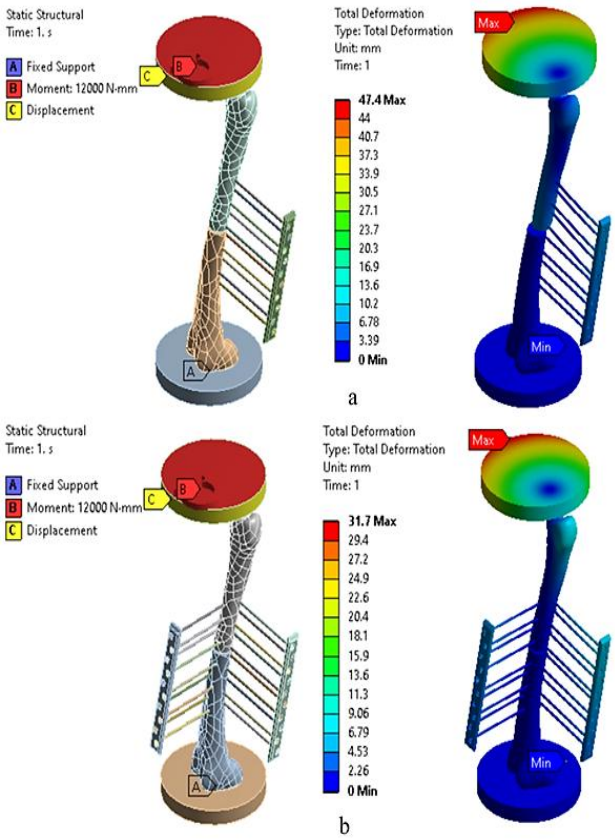

Figure 7. Shows compare a rotation by torsion load applied 12,000 N.mm (a) single LCP, and (b) dual LCP.

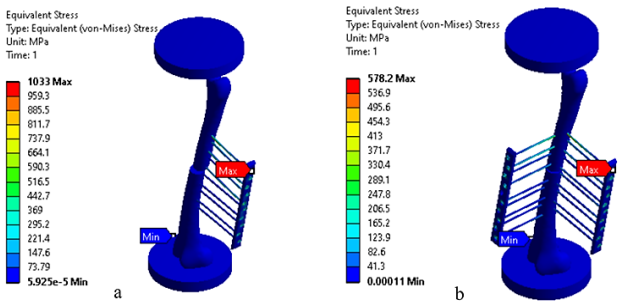

Figure 8. The comparison of the stress by torsion load applied 12,000 N.mm (a) single LCP and (b) dual LCP.

The 4-point bending load was applied for 800 N on the side in the anterior-posterior direction for a femoral bone gap of 3 mm. The anterior-posterior stimulus had a maximum stiffness of dual LCP stiffness higher than a single LCP by considering bone gap fracture size position that a single LCP had a maximum displacement of 3.06 mm and a dual LCP had a maximum displacement of 1.28 mm shown in Fig. 9.

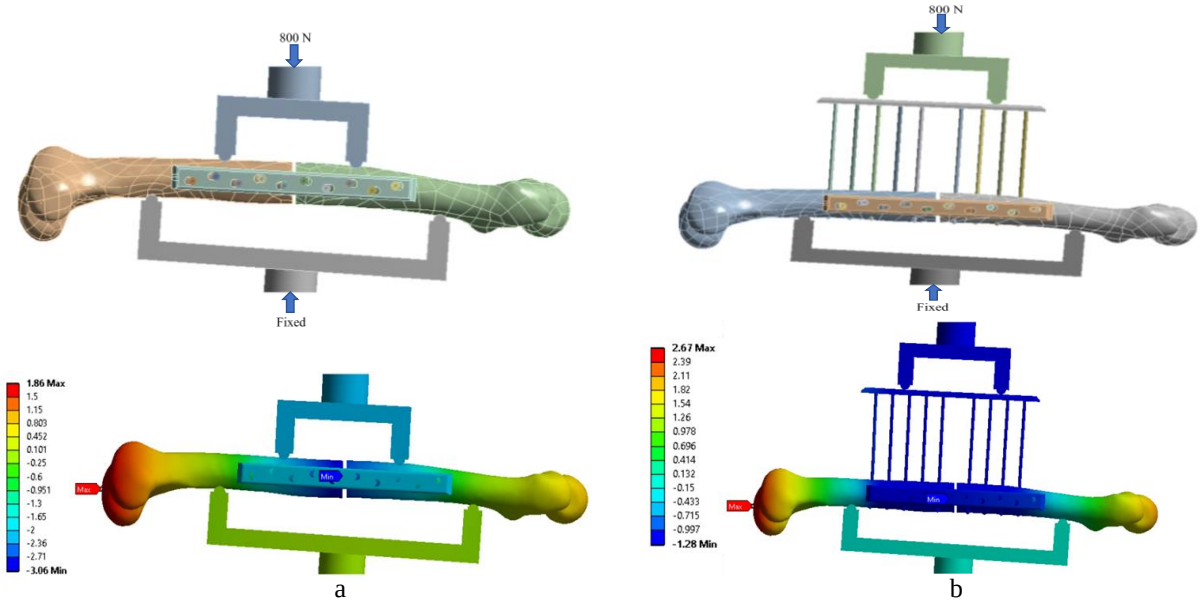

Figure 9. Show deformation of 4-point bending at load 800 N on the anterior-posterior bend in (a) single LCP and (b) dual LCP.

The 4-point bending was loaded for 800 N in the lateral-medial direction for a 3 mm gap fracture of femoral bone which displayed a maximum stiffness in dual LCP which had a displacement on fracture position of 1.90 mm and single LCP had a displacement on fracture position of 1.98 mm shown in Fig. 10.

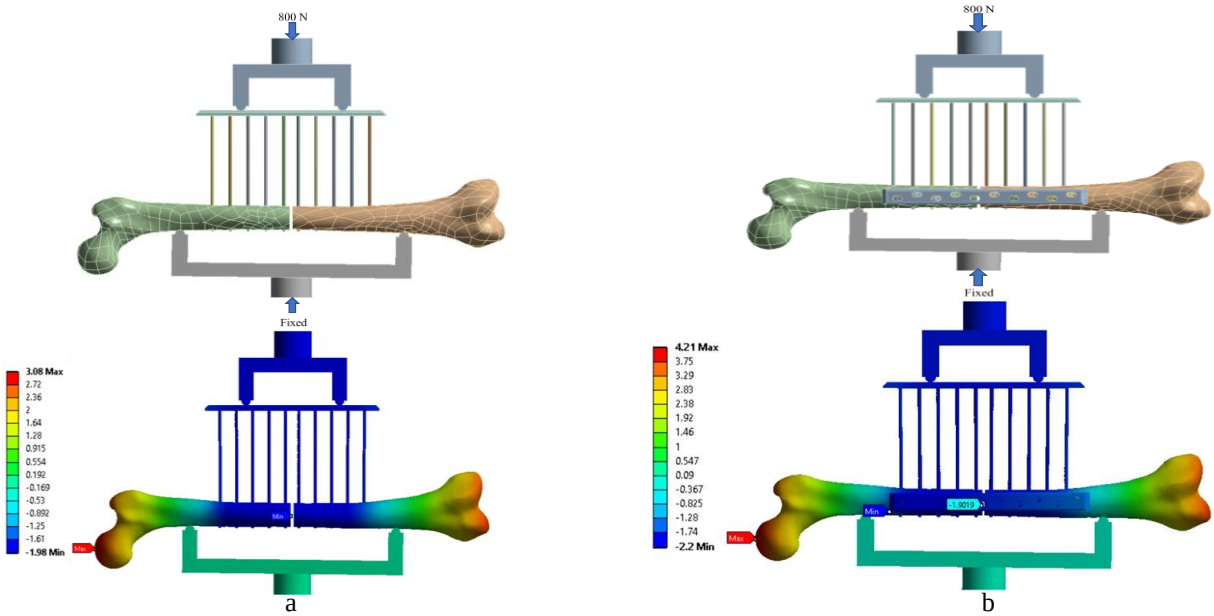

Figure 10. Show deformation of 4-point bending at load 800 N on the lateral-medial bend in (a) single LCP and (b) dual LCP.

The limitations of this study. Firstly, this study used a fresh femoral bone model with individual femoral properties and might have different mechanical properties from the input to calculate stiffness in the FEA model. Secondly, the external fixation with LCP was a variant construct from the external fixation. Muscles and soft tissues envelop affect the outcomes.

This study examined the 10-hole LCP application as an external fixation for a femoral fracture. The calculation for the stiffness of configuration was to compare the stiffness of external fixation that can be used to treat or not to treat. In Fig. 4 the maximum gap was 5 mm for narrow LCP which was a von Misses stress higher than 586 MPa for the ultimate tensile stress of stainless steel 304. A maximum gap of 3 mm for a recheck by stiffness because stiffness was lower than the Unilateral method. The stiffness of 378.55 N.mm/degree by torsion for dual LCP and a single LCP had a stiffness of 253.16 N/degree while a single LCP had maximum stress was 1033 MPa which had stress more than the ultimate tensile stress of stainless steel of 587 MPa thus a single had a deform when torsion load at 12,000 N.mm. The result of a 4-point bending load on the side anterior-posterior had a stiffness of 625 N/mm for a dual LCP and a single LCP with a stiffness of 261.45 N/mm, and the stiffness of a dual LCP had better than a single LCP of 239%. The 4-point bending load on the side lateral-medial had a stiffness of 421.05 N/mm for a dual LCP and a single LCP had a stiffness of 404.04 N/mm, the stiffness of a dual LCP had better than a single LCP of 104%.

As a result of stiffness, a dual LCP for external fixation of femoral bone had stiffness higher than the Unilateral method [2], thus a 10-hole LCP for external fixation may be used clinically if used to double plate. The study of a dual LCP use for external fixation of the femoral which identified a maximum stiffness of 116.45 N/mm compared to the stiffness of the Unilateral method of 107 N/mm was acceptable in safety engineering design [2]. These clinical practices commonly apply for external fixation, which often uses two, three, or four pins to fix the distal and proximal parts of the fracture. An advantage of using FEA was predicting treatment results in the femoral bone fracture model. However, the disadvantage of FEA is that validation with biomechanics testing is required.

IV. Conclusion

Reconstruction found that the stiffness represents the strength of external fixation for femoral bone [1]. FEA is applied to orthopedic surgery to the prognosis of the implant. External fixation of femoral bone is a common treatment for infection in surgery and severe injury of a long bone fracture.

For a gap calculation at the maximum of 5 mm, for 10-hole LCP with the axial load of 800 N, a deformed structure of the implant was found to be better with board LCP than narrow LCP. Recheck torsion load at 12,000 N.mm [6] found that a single LCP was a failure because the maximum von Misses stress had more than the ultimate tensile stress of stainless steel. The bending load on the side of the anterior-posterior was found to be a dual LCP with better stiffness than a single LCP. Dual LCP had a stiffness better than a single LCP by bending load on the side lateral-medial.

However, femur bone fracture treatment with external fixation needs to use a method that had stiffness higher than 107–126 N/mm for external fixation [2]. In this study, a dual LCP was suitable for a treatment surgery femoral bone of external fixation in which a configuration had a strength.

Conflict of Interest

The authors declared no potential conflicts of interest with respect to the research, authorship, and publication of this article.

Author Contributions

Kriengkrai Nabudda and Jarupol Suriyawanakul started to research and create a finite element model and examined the model validation. The manuscript was written by Kriengkrai Nabudda and Kamolsak Sukhonthamarn. Weerachai Kosuwon and Nattadon Pannucharoenwong created methods to implant a model. Kiatfa Tangchaichit supported finite element software for analysis. All authors discussed the results, reviewed, and approved the final version of the manuscript.

Acknowledgment

Professor Yuichi Kasai MD, Ph.D., and Associate Professor Permsak Paholpak MD. have given comments and suggestions in this study.

References

[1] M. Elmedin, A. Vahid, P. Nedim, and R. Nedžad, "Finite element analysis and experimental testing of stiffness of the Sarafix external fixator," *Procedia Engineering*, vol. 100, pp. 1598–1607, 2015.

[2] L. Yang, S. Nayagam, and M. Saleh, "Stiffness characteristics and inter-fragmentary displacements with different hybrid external fixators," *Clinical Biomechanics*, vol. 18, pp. 166–172, 2003.

[3] L. Hidayat, A. F. R. Triangga, C. R. Cein, *et al.*, "Low profile external fixation using locking compression plate as treatment option for management of soft tissue problem in open tibia fracture grade IIIA: A case series," *Int J Surg Case Rep*, vol. 93, Apr, 2022.

[4] Y. Liu, J. Liu, X. Zhang, *et al.*, "Correction outcomes of the postoperative malalignment salvaged by the temporary application of the hexapod external fixator in tibial diaphyseal fractures treated by monolateral external fixation," *Injury*, vol. 52, no. 11, pp. 3478–3482, Nov, 2021.

[5] A. Santoso, H. C. Kumara, S. A. Hadinoto, D. P. A. Prakoso, M. Idulhaq, T. Sumarwoto, and I. Mariyanto, "Acute-shortening and re-lengthening (ASRL) procedure with monorail fixator to treat femur/tibia nonunion: A retrospective study," *Ann Med Surg (Lond)*, vol. 68, 2021.

[6] T. Wisanuyotin, W. Sirichativapee, P. Paholpak, W. Kosuwon, and Y. Kasai, "Optimal configuration of a dual locking plate for femoral allograft or recycled autograft bone fixation: A finite element and biomechanical analysis," *Clin Biomech (Bristol, Avon)*, vol. 80, 2020.

[7] K. Nabudda, J. Suriyawanakul, K. Tangchaichit, *et al.*, "Identification of flexural modulus and poisson's ratio of fresh femoral bone based on a finite element model," *International Journal of Online and Biomedical Engineering (iJOE)*, vol. 18, no. 04, pp. 94–105, 2022.

[8] Y. Kasai, P. Paholpak, K. Nabudda, *et al.*, "Pedicle screw system may not control severe spinal rotational instability," *Spine (Phila Pa 1976)*, vol. 45, no. 21, pp. E1386–E1390, Nov 1, 2020.
[9] O. Refai, and A. A. Khalifa, "Single stage open reduction, intramedullary rod, bone grafting, and plate fixation for managing adolescent midshaft femoral fracture non-union, report of two cases," *Trauma Case Rep*, vol. 38, 2022.
[10] X. Chen, T. E. Andreassen, C. A. Myers, *et al.*, "Impact of periprosthetic femoral fracture fixation plating constructs on local stiffness, load transfer, and bone strains," *J Mech Behav Biomed Mater*, vol. 125, Jan, 2022.
[11] Y. Katz, O. Lubovsky, and Z. Yosibash, "Patient-specific finite element analysis of femurs with cemented hip implants," *Clin Biomech (Bristol, Avon)*, vol. 58, pp. 74–89, Oct, 2018.
[12] J. V. Inacio, A. Malige, J. T. Schroeder, *et al.*, "Mechanical characterization of bone quality in distal femur fractures using pre-operative computed tomography scans," *Clin Biomech (Bristol, Avon)*, vol. 67, pp. 20–26, 2019.
[13] F. Eggermont, G. van der Wal, P. Westhoff, *et al.*, "Patient-specific finite element computer models improve fracture risk assessments in cancer patients with femoral bone metastases compared to clinical guidelines," *Bone*, vol. 130, Jan, 2020.
[14] S. P. Vaananen, L. Grassi, M. S. Venalainen, *et al.*, "Automated segmentation of cortical and trabecular bone to generate finite element models for femoral bone mechanics," *Med Eng Phys*, vol. 70, pp. 19–28, Aug, 2019.
[15] L. Tianye, Y. Peng, X. Jingli, *et al.*, "Finite element analysis of different internal fixation methods for the treatment of Pauwels type III femoral neck fracture," *Biomed Pharmacother*, vol. 112, Apr, 2019.
[16] D. Nolte, and A. M. J. Bull, "Femur finite element model instantiation from partial anatomies using statistical shape and appearance models," *Med Eng Phys*, vol. 67, pp. 55–65, May, 2019.
[17] J. Li, P. Yin, L. Zhang, *et al.*, "Medial anatomical buttress plate in treating displaced femoral neck fracture a finite element analysis," *Injury*, vol. 50, no. 11, pp. 1895–1900, Nov, 2019.
[18] Y. Katz, G. Dahan, J. Sosna, *et al.*, "Scanner influence on the mechanical response of QCT-based finite element analysis of long bones," *J Biomech*, vol. 86, pp. 149–159, Mar 27, 2019.
[19] C. Falcinelli, A. Di Martino, A. Gizzi, *et al.*, "Mechanical behavior of metastatic femurs through patient-specific computational models accounting for bone-metastasis interaction," *J Mech Behav Biomed Mater*, vol. 93, pp. 9–22, May, 2019.
[20] M. T. Bahia, M. B. Hecke, and E. G. F. Mercuri, "Image-based anatomical reconstruction and pharmaco-mediated bone remodeling model applied to a femur with subtrochanteric fracture: A subject-specific finite element study," *Med Eng Phys*, vol. 69, pp. 58–71, Jul, 2019.
[21] M. Marco, E. Giner, R. Larra ńzar-Garijo, *et al.*, "Modelling of femur fracture using finite element procedures," *Engineering Fracture Mechanics*, vol. 196, pp. 157–167, 2018.
[22] I. T. Haider, J. Goldak, and H. Frei, "Femoral fracture load and fracture pattern is accurately predicted using a gradient-enhanced quasi-brittle finite element model," *Med Eng Phys*, vol. 55, pp. 1–8, May, 2018.
[23] E. Dall'Ara, R. Eastell, M. Viceconti, *et al.*, "Experimental validation of DXA-based finite element models for prediction of femoral strength," *J Mech Behav Biomed Mater*, vol. 63, pp. 17–25, Oct, 2016.
[24] I. A. Takacs, A. I. Botean, M. Hardau, and S. Chindris, "Displacement-stress distribution in a femoral bone by optical methods," *Procedia Technology*, vol. 19, pp. 901–908, 2015.
[25] B. Miles, E. Kolos, W. L. Walter, *et al.*, "Subject specific finite element modeling of periprosthetic femoral fracture using element deactivation to simulate bone failure," *Med Eng Phys*, vol. 37, no. 6, pp. 567–573, Jun, 2015.
[26] F. Taddei, I. Palmadori, W. R. Taylor, *et al.*, "European Society of biomechanics S.M. Perren award 2014: Safety factor of the proximal femur during gait: A population-based finite element study," *J. Biomech*, vol. 47, no. 14, pp. 3433–40, Nov 7, 2014.
[27] K. K. Nishiyama, S. Gilchrist, P. Guy, *et al.*, "Proximal femur bone strength estimated by a computationally fast finite element analysis in a sideways fall configuration," *J Biomech*, vol. 46, no. 7, pp. 1231–1236, Apr 26, 2013.
[28] S. Berahmani, D. Janssen, and N. Verdonschot, "Experimental and computational analysis of micromotions of an uncemented femoral knee implant using elastic and plastic bone material models," *J Biomech*, vol. 61, pp. 137–143, Aug 16, 2017.
[29] T. Seechaipat, S. Rooppakhun, and C. Phombut, "Finite element analysis of contact stress distribution on insert conformity design of total knee arthroplasty," *International Journal of Online and Biomedical Engineering (iJOE)*, vol. 18, no. 05, pp. 96–111, 2022.
[30] W. C. Chen, Y. S. Lai, C. K. Cheng, and T.-K. Chang, "A cementless, proximally fixed anatomic femoral stem induces high micromotion with nontraumatic femoral avascular necrosis: A finite element study," *Journal of Orthopaedic Translation*, vol. 2, no. 3, pp. 149–156, 2014.
[31] T. T. Gokhan YUCEL, "Fatigue analysis of welded tubular steel T-joints," *Osmaniye Korkut Ata University Journal of the Institute of Science and Technology*, vol. 5, pp. 1–14, 2022.
[32] T. Tuğrul, "Comparison of nonlinear solution techniques named arc-length for the geometrically nonlinear analysis of structural systems," *Journal of Engg. Research*, vol. 9, pp. 82–109, 2021.
[33] T. Tugrul, "The effect of different strain quantities on behavior of pin-jointed structural systems," *Journal of the Brazilian Society of Mechanical Sciences and Engineering*, vol. 44, no. 8, 2022.